Use of Attenuated Total Internal Reflection−Fourier Transform Infrared Spectroscopy To Investigate the Adsorption of and Interactions between Charged Latex Particles

Robert Kun and Janos H. Fendler*

Department of Chemistry and Center for Advanced Materials Processing, Clarkson University, Potsdam, New York 13699-5814

Received: October 8, 2003; In Final Form: January 20, 2004

The adsorption of 67-, 190-, and 1000-nm-diameter carboxylated latex particles onto hydrophobic and hydrophilic surfaces, from aqueous dispersions of these particles that contain different concentrations of sodium chloride, have been investigated, in situ, by attenuated total internal reflection−Fourier transform infrared spectroscopy. Adsorption of the carboxylated latex particles onto the substrates in a given sample increased exponentially with time and then leveled off to a plateau value (A_{exp}). The value of A_{exp} was dependent on the size of the carboxylated latex particles and on the electrolyte concentration in the dispersions. A_{exp} values were used to calculate the maximum coverage of the substrate by the adsorbed carboxylated latex particles (Θ_{max} values). The Θ_{max} values decreased as the particle size and the ionic strength of the medium decreased. These results were discussed in terms of the product of the Debye length and the radius of the particles (i.e., in terms of the screening parameter, κa).

Introduction

The inherent and fundamental theoretical interest in, and practical importance of, particle deposition, aggregation, and stability have prompted vigorous investigations in this area.[1] Colloidal forces are intimately involved in ceramics,[2] papermaking,[3] filtration technology,[4] mineral processing,[5] paint formulation,[6] food preparation and storage,[7] cosmetics, medical and health-related applications,[8] tertiary oil recovery,[9] pollutant remediation,[10] solar-energy storage and transfer,[11] and high-energy-density batteries.[12] Importantly, the understanding of colloidal forces has significantly contributed to the construction and exploitation of nanostructured materials.[13]

Interaction forces responsible for the stabilities of colloidal particles in aqueous dispersions are generally understood in terms of the Derjaguin, Landau, Verwey, and Overbeek (DLVO) theory, which was proposed some sixty years ago.[14] The stability of a colloidal dispersion is governed, according to the DLVO theory, by a balance between van der Waals attractions and electrostatic double-layer repulsions of the particles. The popularity of the DLVO theory rests upon its success in rationalizing colloidal stabilities and the presence of two aggregation rates: a fast, diffusion-limited rate, which predominates at high salt concentrations or low charge density, and a slow process, which prevails at low electrolyte concentrations or high charge density.

The development of the surface force apparatus,[15] various scanning force microscopies,[16] and optical tweezers[17] for the direct measurement of interaction forces has resulted in the accumulation of a vast body of experimental data that revealed serious disagreements with the DLVO theory, in the slow aggregation regime, at low electrolyte concentrations and at interparticle distances shorter than a few nanometers. Systematic studies have been initiated on the aggregation and sedimentation behavior of well-characterized monodispersed colloidal latex particles, to obtain a quantitative understanding of their behavior. The aggregation has been investigated by simultaneous static and dynamic light scattering,[18] and the sedimentation (onto a variety of different susbtrates) has been examined by transmission electron microscopy (TEM),[19] scanning force microscopy,[20−23] and (IR) infrared spectroscopy.[24]

Here, we report our initial studies on the direct measurements of the time-dependent deposition of well-characterized monodispersed carboxylic latex particles onto hydrophilic and hydrophobic surfaces from aqueous dispersions that contain different concentrations of sodium chloride. The deposition rate of the particles is governed by the mechanism of their transport to the surface of the substrate. This, in turn, is determined by particle−particle and particle−surface interaction forces. For charged particles, the effects of electrolytes on these forces are quantified by the Debye screening length (κ^{-1}). Generally, κ^{-1} and the distance of closest approach between the particles each increase as the ionic strength decreases. This behavior is, in fact, the well-known electrolyte screening effect of charged colloidal particles. Previous investigations of the effects of electrolytes on the deposition of charged silica, hematite, and polystyrene particles onto flat surfaces, glass beads, and large particles followed the expected trend of the product of the Debye length and the radius of the particles (i.e., on the screening parameter, κa) albeit often with large and unexplained discrepancies.[18]

We have monitored the deposition of 67-, 190-, and 1000-nm-diameter carboxylated latex particles, in situ, by attenuated total internal reflection−Fourier transform infrared (ATR−FTIR) spectroscopy. There are several advantages of using ATR−FTIR spectroscopy. First, ATR−FTIR spectrscopy provides a sensitive and accurate means for the in situ determination of the particle concentration at the substrate (the ATR prism) surface in real time. Second, functional groups of the deposited particles can be characterized. Third, it is possible to obtain

* Author to whom correspondence should be addressed. E-mail address: fendler@clarkson.edu.

10.1021/jp037028s CCC: $27.50
Published on Web 02/21/2004

information on depth profiling of the particles, using various angles of the incident IR radiation and of substrates of different refractive indexes.

Experimental Section

Materials. The following chemicals were used as received: surfactant-free, carboxyl-group-functionalized polystyrene latex particles (4.4% (w/v), with mean diameters of 1000, 190, and 67.0 nm (batch numbers 1720, 1892/1, and 520/1, respectively, Interfacial Dynamics Corp., Portland, OR)); sodium chloride and sulfuric acid (Fisher Scientific, Fairlawn, NJ); absolute ethanol (Pharmco, Brookfield, CT); potassium chromate (Baker and Adamson, Morristown, NJ); and methanol (99.9% (v/v)) and (3-mercaptopropyl)-trimethoxysilane, 95% (v/v) (each from Aldrich Chemical, Inc., Milwaukee, WI). Ultrapure water, with a resistivity of >18 MΘ cm, were prepared using a Millipore Milli-Q column system that was provided with a Milli-pak filter (pore size of 0.22 μm) at the outlet.

Germanium prisms (surface dimensions 15 mm × 25 mm, Macrooptica, Moscow, Russian Federation) were cleaned with absolute ethanol and Milli-Q water before and after each experiment. In some cases, the prism was polished to remove the adsorbed latex layer from the germanium surface, via chemical mechanical polishing, using 150-nm-mean-diameter amorphous silica particles in aqueous dispersion and a SUBA 500 Pad (polyurethane-impregnated polyester felt, Rodel Co., Wilmington, DE).

All glassware and vials, as well as the cell, were scrupulously cleaned prior to use by freshly made chromic acid (sulfuric acid that had been saturated with potassium chromate at 25 °C) and then copiously rinsed with Milli-Q water.

Experimental Procedure. The carboxylated latex particle dispersions were diluted by aqueous sodium chloride solutions to give the desired concentrations of the electrolyte in the samples. Carboxylated latex particle concentrations were kept constant at 0.44% (w/v) in all samples (with the exception of a couple of measurements using 0.22% (w/v) carboxylated latex particles). No buffers or any other additives were used. The samples were stored in a refrigerator at all times, at temperatures of 5−8 °C; however, immediately before analysis, the actual sample was brought to and kept at room temperature for 2 h. The pH values of these samples, determined before and after the sedimentation experiments, varied in the range of 5.50−6.10. All measurements were performed at ambient temperature and atmosphere.

The sedimentation experiments were conducted in a homemade glass cell, that had been immobilized on top of the substrate (the germanium ATR prism) by a cell holder and a rubber "O"-ring 0.80 cm in diameter (Figure 1), which was attached to a modified Digilab Universal Reflection Accessory. The prism position and the angle of the mirrors were then adjusted manually to maximize the interferogram signal of the FTIR instrument. The entire measurement stage was turned upside down (to provide a configuration in which the particles could settle horizontally onto the prism surfaces, as shown in Figure 1) when the maximum signal was reached and the adjustment was repeated. Eventually, the signal reached a value of 6.9−7.1, using an open aperture. To record the background spectra, 400 μL of Milli-Q water was injected gently into the cell (to avoid forming an air bubble on the germanium surface), by means of a Teflon tube, which was closed by glass stoppers. This procedure was followed by the closing of the sample compartment, the purging of the chamber by purified air for 2 h (to minimize the CO_2 and water-vapor content in the instrument), and the recording of the background (water in the cell) spectra. Water was then sucked out gently from the cell by the Teflon tube (taking care not to alter the alignment of the cell). Homogenized 400-μL-diameter aqueous carboxylated latex particle dispersion (at the desired electrolyte concentration) was then carefully introduced into the cell by the Teflon tube, and sample spectra were repeatedly recorded every 20 min for 8 h (or until the absorption spectrum no longer increased). The final absorbance data were scanned after 20−25 h of deposition, depending on the sample. Typically, 256 interferograms were co-added to record each spectrum, which required ∼5 min. Experiments were performed in triplicate for the 1000- and 67-nm-diameter carboxylated latex particles and in duplicate for the 190-nm-diameter particles. The average deviation of the absorbance for a sample was calculated to be ±5%.

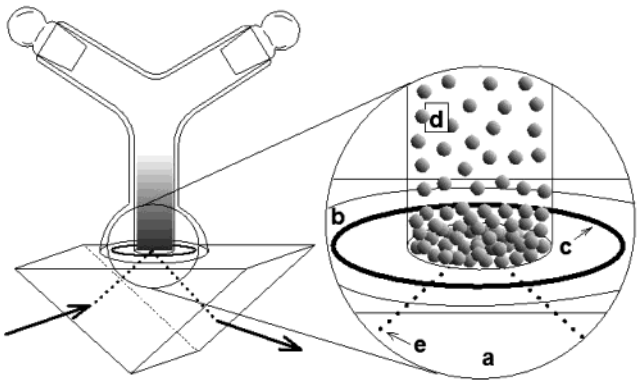

Figure 1. Schematic of the cell used for the investigation of carboxylated latex particle adsorption. Legend is as follows: a, germanium prism; b, bottom of the glass cell; c, "O"-ring; d, aqueous dispersion of the carboxylated latex particles; and e, infrared beam. For clarity, the cell holder is not shown.

The transmission FTIR measurements of the aqueous carboxylated latex particle dispersions were performed in a solution cell that had 10-mm-diameter CaF_2 windows and 15-μm-thick Teflon spacers (Wilmad, Buena, NJ), using pure Milli-Q water for the background.

The largest surface of the germanium prism was rendered hydrophobic via derivatization by 3-mercaptopropyl)-trimethoxysilane (incubating it in a mixture of methanol and 3-mercaptopropyl)-trimethoxysilane, 1:4 = v:v, overnight and rinsing it copiously using Milli-Q water).

Instrumentation. The pH values of the carboxylated latex particle dispersions were determined using a pH meter (ThermoOrion model 525A+) and a combination glass electrode (Corning Incorporated Life Sciences). Prior to each measurement, the electrode was calibrated by two standard buffers (pH = 4.00 and pH = 10.00).

All the ATR−FTIR spectral analyses were performed on a spectrometer (Digilab model FTS7000) that used a globar tungsten halogen source and a DTGS detector. The aperture (open), resolution (4 cm^{-1}), undersampling ratio (UDR = 2), and sensitivity (1) were the same in all experiments. A variable-angle twin-parallel-mirrors accessory and a homemade cell holder were used in each experiment. The deposition of the latex particles was monitored through the use of BioRad Win-IR Pro 3.1 software, using the Timed Collect method.

Theoretical Section

The calculations are based on a three-phase stratified medium, namely, (1) the prism, (2) the monoparticulate layer of adsorbed carboxylated latex particles, and (3) the aqueous carboxylate

latex particle dispersion. The absorbance due to the asymmetric CH_2 vibration (A) is directly related to the concentration of the absorbing species, $C(z)$, and is expressed as

$$A = \int_0^\infty \frac{(n_3/n_1)E_0^2\epsilon C(z)}{\cos(\pi\theta/180)} \exp\left(-\frac{2z}{d_p}\right) dz \qquad (1)$$

where n_1 and n_3 are the refractive indexes of the prism (4.0) and the aqueous carboxylate latex particle dispersion (1.59), respectively; ϵ is the molar absorptivity of the CH_2 vibration of the carboxylated latex particles (2597.7 M^{-1} cm^{-1}; see the Results and Discussion section) at the observed wavelength λ ($\lambda = 3422.3$ nm); E_0 is the relative average electric field at the interface; I is the incident angle (46.25°); and d_p is the penetration depth of the IR radiation (225.8 nm) and is determined by

$$d_p = \frac{\lambda/n_1}{2\pi\sqrt{\sin^2\left(\frac{\pi\theta}{180}\right) - \left(\frac{n_1}{n_2}\right)^2}} \qquad (2)$$

Note that eq 1 is integrated from the interface to infinity; thus, this integration is the sum of the contributions of the bulk aqueous colloidal particle dispersion and monoparticulate layer of carboxylated latex particles adsorbed on the prism if the penetration depth of the evanescent wave is greater than the mean diameter of the latex particles (r, in nanometers). The absorbance of the latex particles dispersed in the aqueous bulk solution is given by

$$A_v = \int_{2r}^\infty \frac{(n_3/n_1)E_0^2\epsilon C_b}{\cos(\pi\theta/180)} \exp\left(-\frac{2z}{d_p}\right) dz \qquad (3)$$

where C_b is the concentration profile of the absorbing species in the dispersion and z is the perpendicular distance from the prism that encompasses the volume of the dispersed carboxylated latex particles. If the diameter of the latex particles is less than the penetration depth, the integration limits should be from zero to half of the penetration depth. The penetration depth (d_p) represents the distance at which the electric-field amplitudes have decayed to $1/e$ of their intensity at the interface. However, the absorbance is proportional to the square of these amplitudes and decays to $1/e$ of its value at the interface half of this distance, and we used, therefore, $d_p/2$ as the upper integration limit for expressing the absorbance of the monoparticulate layer of carboxylated latex particles adsorbed onto the prism:

$$A_{exp} = \int_0^{2r \text{ or } d_p/2} \frac{(n_3/n_1)E_0^2\epsilon C_1(z)}{\cos(\pi\theta/180)} \exp\left(-\frac{2z}{d_p}\right) dz \qquad (4)$$

where $C_1(z)$ is the concentration profile of the absorbing species within the monoparticulate layer along the z-direction.

The experimentally measured absorbance is

$$A_{exp} = A_1 + A_v \quad (\text{for } d_p > 2r) \qquad (5a)$$

$$= A_1 \quad (\text{for } d_p < 2r) \qquad (5b)$$

A_1 is the sum of the absorbances of all particles on the substrate in the irradiated area S. If the contribution of one particle is A_{10}, the number of particles (N) on the substrate in the irradiated area should be

$$N = \frac{A_1}{A_{10}} = \frac{A_{exp} - A_v}{A_{10}} \quad (\text{for } d_p > 2r) \qquad (6a)$$

$$= \frac{A_{exp}}{A_{10}} \quad (\text{for } d_p < 2r) \qquad (6b)$$

Knowing the values for C_b and C_1, the value of N can be obtained. Hence, the maximum coverage of the substrate by the adsorbed carboxylated latex particles (Θ_{max}) is given by

$$\Theta_{max} = \frac{N(\pi r^2)}{S} = \frac{\pi r^2(A_{exp} - A_v)}{SA_{10}} \quad (\text{for } d_p > 2r) \qquad (7a)$$

$$= \frac{\pi r^2 A_{exp}}{SA_{10}} \quad (\text{for } d_p < 2r) \qquad (7b)$$

In eqs 3 and 4, the parameters n_1, n_2, n_3, d_p, C_b, ϵ, E_0, r, and I are known; only $C_1(z)$ is unknown. Suppose that the absorbing species are uniformly distributed with a molar concentration p. To obtain the variation of the concentration of the species along the z-direction, it is convenient to affect a mathematical transformation of spherical to cylindrical particles (Figure 2). This transformation implies the same height ($2r = L$), the same volume ($^4/_3\pi r^3 = \pi r^2 L$), and same molar amounts of absorbing species of the spherical and cylindrical particles at the same distance z from the substrate: $\rho\pi(2rz - z^2) = \rho_0(z)\pi r^2$. The number of species is proportional to the area ($2rz - z^2$) of the cross section perpendicular to the substrate (i.e., the z-direction, as shown in Figure 2). The concentration profile of absorbing species is then obtained as

$$\rho_0 = \rho\left[\frac{3(2zr - z^2)}{2r^2}\right] \qquad (8)$$

where ρ is the molar concentration of the polystyrene in an equivalent cylinder or pillar and ρ_0 is the molar concentration of polystyrene in a particle (both expressed per monomer in units of mol/L). Suppose that there are N number of cylindrical particles in the irradiated area of the substrate (S); then, the area coverage is $N\pi r_0^2/S$, and the concentration of absorbing species of a monoparticulate layer is

$$C_1(z) = \rho_0\frac{N\pi r_0^{\,2}}{S} = \rho\left[\frac{N\pi(2zr - z^2)}{S}\right] \qquad (9)$$

Therefore, the contribution of each cylindrical particle to the concentration of species within the monoparticulate layer is

$$C_{10}(z) = \rho\left[\frac{\pi(2zr - z^2)}{S}\right] \qquad (10)$$

and the contribution of each particle to the absorbance of the species within this monoparticulate layer is

$$A_{10} = \int_0^{2r \text{ or } d_p/2} \frac{(n_3/n_1)E_0^2\epsilon C_{10}(z)}{\cos(\pi\theta/180)} \exp\left(-\frac{2z}{d_p}\right) dz \qquad (4a)$$

and introducing $C_{10}(z)$ (from eq 10) leads to

$$A_{10} = \int_0^{2r \text{ or } d_p/2} \left[\frac{(n_3/n_1)E_0^2\epsilon}{\cos(\pi\theta/180)}\right]\rho\left[\frac{\pi(2rz - z^2)}{S}\right] \exp\left(-\frac{2z}{d_p}\right) dz \qquad (11)$$

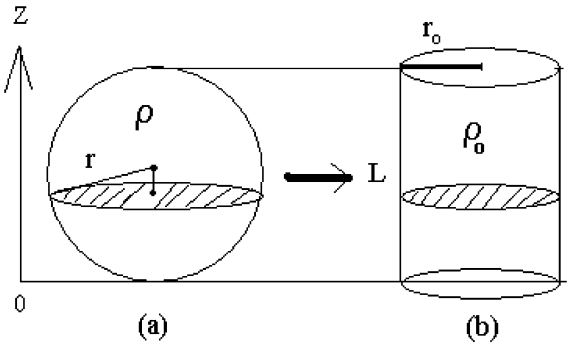

Figure 2. Schematic of the mathematical transformation of spherical particles to cylindrical particles (see text, "Theoretical Section").

Returning to eq 7 and using eq 11 yields the following:

$$\Theta_{max} = \frac{r^2(A_{exp} - A_v)}{\int_0^{2r} \frac{(n_3/n_1)E_0^2\epsilon}{\cos(\pi\theta/180)}\rho(2rz - z^2)\exp\left(-\frac{2z}{d_p}\right)dz} \quad (\text{for } 2r > d_p) \quad (12)$$

$$\Theta_{max} = \frac{r^2 A_{exp}}{\int_0^{d_p/2} \frac{(n_3/n_1)E_0^2\epsilon}{\cos(\pi\theta/180)}\rho(2rz - z^2)\exp\left(-\frac{2z}{d_p}\right)dz} \quad (\text{for } 2r > d_p) \quad (13)$$

From eqs 12 and 13, we can see that, in our calculations, it is not necessary to know the area of the IR light beam on the substrate (*S*)!

Finally, the interparticle distances h_p between the carboxylated latex particles adsorbed on the prism can be estimated by assuming either a random sequential adsorption (RSA) or a ballistic model for the deposition of the particles:

$$h = r\left(\sqrt{\frac{0.547}{\text{coverage}}} - 1\right) \quad \text{(RSA model)} \quad (14)$$

$$h = r\left(\sqrt{\frac{0.611}{\text{coverage}}} - 1\right) \quad \text{(ballistic model)} \quad (15)$$

Results and Discussion

The characteristic asymmetric CH_2 vibrational band manifested itself at 2922 cm^{-1} in the ATR−FTIR spectra of the 1000-, 190-, and 67-nm-diameter carboxylated latex particles, adsorbed from an aqueous 0.10 M NaCl dispersion onto the surface of the germanium prism (Figure 3). Furthermore, with time, the area of this absorption band was observed to increase for a given sample, which indicated the adsorption of an increasing number of carboxylated latex particles onto the substrate surface (i.e., onto the germanium prism). Identical spectra were obtained in the transmission mode (in a solution cell) for aqueous dispersions of the carboxylated latex particles (see Figure 3). Using the intensities of the absorption maximum at 2922 cm^{-1} at different carboxylated latex particle concentrations (0.22%, 0.44%, 1.10% (w/v)) in 0.05 M NaCl led to a molar absorptivity (ϵ) of 2597.7 M^{-1} cm^{-1}, which was the value used in all of our calculations (eq 1).

Adsorption of the carboxylated latex particles onto the germanium surface in a given sample increased exponentially with time and then leveled off to a plateau value, A_{exp} (Figure 4). This plateau value remained unchanged for several days. The rate needed to reach A_{exp} was dependent on the concentration of the carboxylated latex particles in the dispersion. At higher carboxylated latex particle concentrations, less time was required to reach A_{exp}. However, at a given electrolyte concentration, the same plateau value of adsorption (i.e., A_{exp}) was obtained for different concentrations of identically sized carboxylated latex particles, as expected for a true saturation plateau. This is illustrated in Table 2 for 0.44% (w/v) and 2.2% (w/v) 190-nm-diameter carboxylated latex particles in 0.100 M NaCl. Values of A_{exp} for 0.44% (w/v) 1000-, 190-, and 67-nm-diameter carboxylated latex particles in different NaCl concentrations are collected in Tables 1, 2, and 3, respectively.

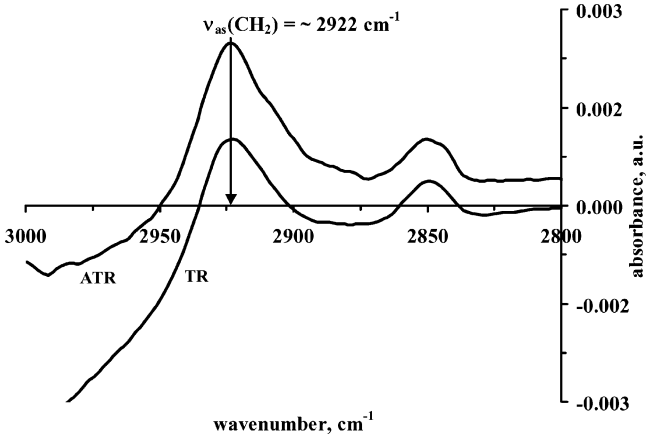

Figure 3. ATR−FTIR spectrum (ATR) of 0.44% (w/v) carboxylated latex particles in 0.05 M aqueous NaCl solution 480 min after their introduction into the cell shown in Figure 1. For comparison, the transmission spectrum (TR) of an aqueous 0.44% (w/v) carboxylated latex particle dispersion in 0.05 M NaCl is also shown.

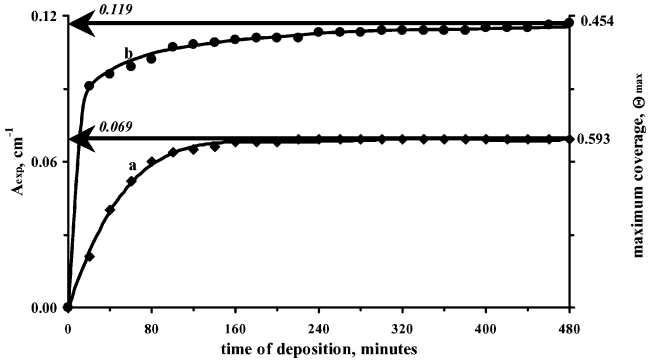

Figure 4. Adsorption of 0.44% (w/v) carboxylated latex particles ((a) 1000-nm-diameter and (b) 190-nm-diameter) dispersed in 0.1 M NaCl, as a function of time.

Taking advantage of eqs 12 and 13, we calculated the maximum coverage of the substrate by the adsorbed carboxylated latex particles (Θ_{max} values) and collected them into Tables 1−3. Tables 1−3 also include the calculated interparticle distances on the substrate surface, the Debye screening length (κ^{-1}), and values for the screening parameter (κa) for the 1000-, 190-, and 67-nm-diameter carboxylated latex particles. The Θ_{max} values follow two previously reported trends.[18] First, the maximum coverage of the substrate surface was observed to decrease as the particle size decreased. For example, in 0.100 M NaCl, the Θ_{max} values were 0.593 (Table 1), 0.454 (Table 2), and 0.392 (Table 3) for the 1000-, 190-, and 67-nm-diameter carboxylated latex particles, respectively. Second, decreasing the ionic strength of the medium in which a given sized carboxylated latex particle is dispersed resulted in decreased surface coverage (see Tables 1−3).

Particle deposition has been rationalized in terms of simple geometrical packing considerations, transport to the substrate

TABLE 1: Deposition of 1000-nm-Diameter Carboxylated Latex Particles

[NaCl] (M)[a]	pH[b]	A_{exp} (cm^{-1})[c]	maximum coverage, Θ_{max}[d]	Interparticle Distance, h (nm)		M (nm^{-1})[e]	κa[f]
				ballistic model (eq 15)	RSA model (eq 14)		
0.100	5.62	0.069	0.593	15.4		0.720	363
0.050	5.53	0.068	0.584	22.8		0.513	257
0.010	5.64	0.039	0.335	351	278	0.229	115
0.005	6.33	0.023	0.198	759	664	0.162	81.2
0.001	5.70	0.011	0.0945	1540	1410	0.0726	36.3

[a] The concentration of carboxylated latex particles was kept at 0.44% (w/v). [b] Mean of measured pH values. [c] Area of the absorption peak, due to the CH_2 vibrations of the carboxylated latex particles, calculated by eq 5 from the data observed at saturation coverage at an angle of incidence of $\Theta_1 = 46.25°$, a critical angle of $\alpha = 23.42°$, and a penetration depth of $d_p = 226$ nm. The experiments were performed in triplicate, and, for each value, the average deviation for each value was calculated to be ±5%. [d] Values calculated from eq 13. [e] Debye length, calculated from $\kappa = e\sqrt{C_0/(\epsilon_0\epsilon_r kT)}$, where e is the elementary charge ($e = 1.602 \times 10^{-19}$ C), C_0 the concentration of the electrolyte (in m^{-3}, because $C_0 = cN_A$, where c is the molar concentration of the electrolyte in mol m^{-3} and N_A is Avogadro's constant), ϵ_0 the permittivity in a vacuum ($\epsilon_0 = 8.854 \times 10^{-12}$ C $(V\ m)^{-1}$), ϵ_r the relative dielectric permittivity of the carboxylated latex particles (taken to be $\epsilon_r = 80$), k the Boltzmann's constant ($k = 1.381 \times 10^{-23}$ J/K), and T the absolute temperature ($T = 300$ K). [f] Screening parameter $= \kappa a$, where a is the radius of the carboxylated latex particles (in meters) and κ is given in units of m^{-1}.

TABLE 2: Deposition of 190-nm-Diameter Carboxylated Latex Particles

[NaCl] (M)[a]	pH[b]	A_{exp} (cm^{-1})[c]	maximum coverage, Θ_{max}[d]	Interparticle Distance, h (nm)		M (nm^{-1})[e]	κa[f]
				ballistic model (eq 15)	RSA model (eq 14)		
0.200	6.32	0.131	0.505	19.1	7.82	1.030	97.5
0.100	6.39	0.119	0.454	30.3	18.5	0.726	69.0
0.100[g]	6.39	0.119	0.454	30.3	18.5	0.726	69.0
0.100[h]	6.39	0.119	0.454	30.3	18.5	0.726	69.0
0.050	6.71	0.0888	0.339	65.2	51.5	0.513	48.8
0.040	6.37	0.0824	0.314	75.1	60.9	0.459	43.6
0.030	6.48	0.0751	0.285	88.0	73.1	0.398	37.8
0.025	6.69	0.0531	0.200	142	124	0.363	34.5

[a] The concentration of carboxylated latex particles was kept at 0.44% (w/v), unless stated otherwise. [b] Mean of measured pH values. [c] Area of the absorption peak, due to the CH_2 vibrations of the carboxylated latex particles, calculated by eq 5 from the data observed at saturation coverage at an angle of incidence of $\Theta_1 = 46.25°$, a critical angle of $\alpha = 23.42°$, and a penetration depth of $d_p = 225.76$ nm. The experiments were performed in duplicate, and the average deviation for each value was calculated to be ±5%. [d] Values calculated from eq 12. [e] Debye length, calculated from $\kappa = e\sqrt{C_0/(\epsilon_0\epsilon_r kT)}$, where e is the elementary charge ($e = 1.602 \times 10^{-19}$ C), C_0 the concentration of the electrolyte (in m^{-3}, because $C_0 = cN_A$, where c is the molar concentration of the electrolyte in mol m^{-3} and N_A is Avogadro's constant), ϵ_0 the permittivity in a vacuum ($\epsilon_0 = 8.854 \times 10^{-12}$ C $(V\ m)^{-1}$), ϵ_r the relative dielectric permittivity of the carboxylated latex particles (taken to be $\epsilon_r = 80$), k the Boltzmann's constant ($k = 1.381 \times 10^{-23}$ J/K), and T the absolute temperature ($T = 300$ K). [f] Screening parameter $= \kappa a$, where a is the radius of the carboxylated latex particles (in meters) and κ is given in units of m^{-1}. [g] Using a silanated (hydrophobic) germanium surface. [h] Using 2.2% (w/v) carboxylated latex particles.

TABLE 3: Deposition of 67-nm-Diameter Carboxylated Latex Particles

[NaCl] (M)[a]	pH[b]	A_{exp} (cm^{-1})	maximum coverage, Θ_{max}[d]	Interparticle Distance, h (nm)		M (nm^{-1})[e]	κa[f]
				ballistic model (eq 15)	RSA model (eq 14)		
0.200	5.71	0.0930	0.596	0.83		1.03	34.4
0.150	5.85	0.0840	0.535	4.61	0.76	0.889	29.8
0.100	6.02	0.0630	0.392	16.67	12.17	0.726	24.3
0.050	5.93	0.0370	0.215	46.02	39.94	0.513	17.2

[a] The concentration of carboxylated latex particles was kept at 0.44% (w/v). [b] Mean of measured pH values. [c] Area of the absorption peak, due to the CH_2 vibrations of the carboxylated latex particles, calculated by eq 5 from the data observed at saturation coverage at an angle of incidence of $\Theta_1 = 46.25°$, a critical angle of $\alpha = 23.42°$, and a penetration depth of $d_p = 225.76$ nm). The experiments were performed in triplicate, and, for each value, the average deviation was calculated to be ±5%. [d] Values calculated from eq 12. [e] Debye length, calculated from the equation $\kappa = e\sqrt{C_0/(\epsilon_0\epsilon_r kT)}$, where e is the elementary charge ($e = 1.602 \times 10^{-19}$ C), C_0 the concentration of the electrolyte in m^{-3}, because $C_0 = cN_A$, where c is the molar concentration of the electrolyte in mol m^{-3} and N_A is Avogadro's constant), ϵ_0 the permittivity in a vacuum ($\epsilon_0 = 8.854 \times 10^{-12}$ C $(V\ m)^{-1}$), ϵ_r the relative dielectric permittivity of the carboxylated latex particles (taken to be $\epsilon_r = 80$), k the Boltzmann's constant ($k = 1.381 \times 10^{-23}$ J/K), and T the absolute temperature ($T = 300$ K). [f] Screening parameter $= \kappa a$, where a is the radius of the carboxylated latex particles (in meters) and κ is given in units of m^{-1}.

surface, particle−particle, particle−solvent, and particle−surface interactions. Simple packing of particles onto the substrate surface was modeled by the RSA model and ballistic deposition. In the RSA model, the sequential deposition of the particles starts from an empty surface and continues until the "jamming limit" is attained (i.e., no more space is available), such that no overlap occurs during the deposition.[25] In the ballistic model, none of the incoming particles are rejected; they are free to continue in their downward path of the steepest descent until they reach a stable position.[26] Particles reaching the substrate surface are accepted, and those which come to rest on top of previously adsorbed particles are rejected. After a particle is deposited on the substrate surface, it is assumed to not to move or be removed. No consideration was given to particle−particle and particle−surface interactions in the presence of electrolytes in these simple models. The surface coverage in the RSA and ballistic models were calculated to be 54.7% and 61.1%, respectively. Note that, for the 1000-nm-diameter carboxylated latex particles, the maximum surface coverage in 0.100 M NaCl (0.593, in Table 1) is almost as high as that predicted by the

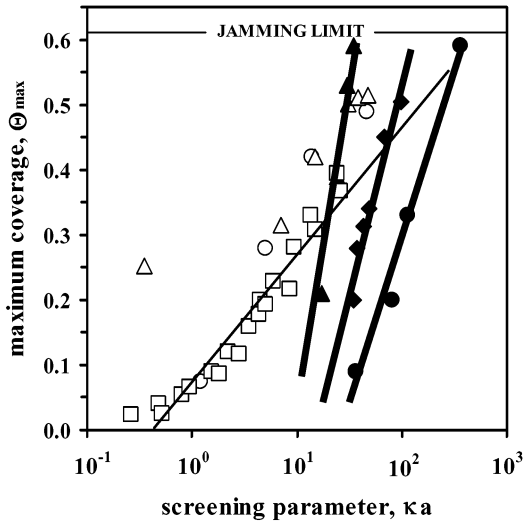

Figure 5. Plot of the maximum surface coverage (Θ_{max}) of the adsorbed (●) 1000-nm , (◆) 190-nm and (▲) 67-nm-diameter carboxylated latex particles against the screening parameter (κa). The empty symbols represent data taken from the published literature: (○) negatively charged 470-nm-radius polystyrene sulfate latex particles adsorbed onto positicely charged treated mica,[29] (△) negatively charged 72-nm-radius polystyrene sulfate latex particles adsorbed onto positively treated glass,[30] and (□) negatively charged silica particles (radius of 9−45 nm) adsorbed onto positively charged polyvinylimidazole-covered Si/SiO_2.[31] The solid line is drawn to guide the eye through the silica series of data (□ symbols).

ballistic model and, in fact, is higher than that calculated by the RSA model. Recall that no charge interactions were considered in the simple RSA or ballistic models.

It was Adamczyk and co-workers who first formulated analytical expressions for the kinetics of charged colloidal particle deposition and for the maximum surface concentration (Θ_{max} in our terminology) of the adsorbed particles by including electrostatic interactions in the simple RSA model.[18,27] Following previous work,[18] we have plotted Θ_{max} values for the 1000-, 190-, and 67-nm-diameter carboxylated latex particle adsorption onto the germanium substrate surface in the presence of different electrolytes against the screening parameter κa (Figure 5). Within the range investigated, plots of the Θ_{max} value against κa were determined to be linear for the differently sized particles (see broad lines in Figure 5), although the size differences were somewhat larger than those previously observed for positively charged latex particles.[18] As expected, the maximum coverage at a given κa value progressively increased as the diameter of the carboxylated latex particles decreased.[28] However, we did not investigate the adsorption of the smallest particles at very low ionic strength (i.e., in the region where the κa values are in the range of 0.1−1.0). In Figure 5, we have also included data points from previous investigations of the adsorptions of anionic polystyrene sulfate latex particles on positively treated mica and glass surfaces, as well as for the adsorption of negatively charged silica particles on cationically charged polyvinylimidazole-covered Si/SiO_2 surfaces. Although the trend in the previous values is quite similar to that observed here, they generally show a maximum surface coverage at lower κa values. Differences in the particles and the techniques used are likely to be responsible for these discrepancies.

Interestingly, in a preliminary investigation of the deposition of 190-nm-diameter carboxylated latex particles from their dispersion in aqueous 0.100 M NaCl, we observed identical maximum coverages of a hydrophobically treated substrate and the untreated hydrophilic germanium substrate (see Table 2).

Demonstration of the use of ATR−FTIR to monitor the in situ adsorption of small and large colloidal particles from their aqueous electrolyte dispersions and the treatment of the obtained data, to shed light upon particle−particle and particle−substrate interactions, is the most significant result of the present work. It opens the door for more in-depth investigations of colloidal interactions in many other systems via this approach.

Acknowledgment. We thank the U.S. Department of Energy for supporting this work.

References and Notes

(1) Evans, D. F.; Wennerstrom, H. *The Colloidal Domain Where Physics, Chemistry and Technology Meet*; VCH Publishers: New York, 1999.

(2) (a) Gauckler, L. J.; Graule, T.; Baader, F. *Mater. Chem. Phys.* **1999**, *61*, 78. (b) Balzer, B.; Hruschka, M. K. M.; Gauckler, L. J. *J. Colloid Interface Sci.* **1999**, *216*, 379.

(3) (a) Horn, D. In *Polymeric Amines and Ammonium Salts*; Goethals, E. J., Ed.; Pergamon Press: Oxford, U.K., 1980. (b) van de Ven, T. G. M.; Alince, B. *J. Colloid Interface Sci.* **1996**, *181*, 73.

(4) (a) Jewett, D. G.; Hilbert, T. A.; Logan, B. E.; Arnold, R. G.; Bales, R. C. *Water Res.* **1995**, *29*, 1673. (b) Song, L.; Elimelech, M. *J. Chem. Soc., Faraday Trans.* **1995**, *91*, 3389.

(5) (a) Pugh, R. J. In *Surface and Colloid Chemistry in Advanced Ceramics Processing*; Pugh, R. J., Bergstrom, L., Eds.; Marcel Dekker: New York, 1994. (b) Bustamante, H.; Rutter, P. R. *Chem. Eng. Sci.* **1987**, *42*, 809. (c) Moudgill, B. M.; Behl, S. In *Flotation Science and Engineering*; Matis, K. A., Ed.; Marcel Dekker: New York, 1995. (d) McLaughlin, W. J.; White, J. L.; Hem, S. L. *J. Colloid Interface Sci.* **1994**, *167*, 74.

(6) (a) Nabuurs, T.; Baijards, R. A.; German, A. L. *Prog. Org. Coat.* **1996**, *27*, 163. (b) Verkholantsev, V. V. *J. Coat. Technol.* **1996**, *68*, 49.

(7) Dickinson, E. *Trends Food Sci. Technol.* **1997**, *8*, 334.

(8) (a) Aikens, P.; Friberg, S. E. *Curr. Opin. Colloid Interface Sci.* **1996**, *1*, 672. (b) Ouali, L.; Pefferkorn, E.; Elaissari, A.; Pichot, C.; Mandrand, B. *J. Colloid Interface Sci.* **1995**, *171*, 276.

(9) (a) Schumacher, M. M., Ed. *Enhanced Oil Recovery: Secondary and Tertiary Methods*; Noyes Data Corp.: Park Ridge, NJ, 1978. (b) Pope, G. A.; Wade, W. H. In *Surfactant-Enhanced Subsurface Remediation: Emerging Technologies*; Sabatini, D. A., Knox, R. K., Harwell, J. H., Eds.; American Chemical Society: Washington, DC, 1995; p. 1. (c) Ding, R.; Qiu, Z.; Li, J. *Oil Gas J.* **1996**, *94*, 66.

(10) (a) Kretzschmar, R.; Barmettler, K.; Grolimund, D.; Yan, Y. D.; Borkovec, M.; Sticher, H. *Water Resour. Res.* **1997**, *33*, 1129. (b) Okahata, Y.; Yokobori, M.; Ebara, Y.; Ebato, H.; Ariga, K. *Langmuir* **1990**, *6*, 1148. (c) Litton, G. M.; Olson, T. M. *Environ. Sci. Technol.* **1993**, *27*, 185. (d) Jin, Y.; Yates, M. V.; Thompson, S. S.; Jury, W. A. *Environ. Sci. Technol.* **1997**, *31*, 548.

(11) (a) Gratzel, M. *Curr. Opin. Colloid Interface Sci.* **1999**, *4*, 314. (b) Heath, J. R. *Acc. Chem. Res.* **1999**, *32*, 388.

(12) (a) Wakihara, M., Yamamoto, O., Eds. *Lithium Ion Batteries: Fundamentals and Performance*; Kodansha, Wiley−VCH: Weinheim, Germany, 1998. (b) Owen, J. R. *Chem. Soc. Rev.* **1997**, *26*, 259. (c) Kotov, N. A.; Dekany, I.; Fendler, J. H. *Adv. Mater.* **1996**, *8*, 637.

(13) *Small Wonders, Endless Frontiers—A Review of the National Nanotechnology Initiative*; National Academy Press: Washington, DC, 2002. (Also can be obtained via the Internet at www.nano.gov.)

(14) (a) Derjaguin, B. V.; Landau, L. *Acta Physicochim. USSR* **1941**, *14*, 633. (b) Verwey, E. J. W.; Overbeek, J. T. G. *Theory of Stability of Lyophobic Colloids*; Elsevier: Amsterdam, 1948.

(15) (a) Israelachvili, J. N. *Surf. Sci. Rep.* **1992**, *14*, 109−159. (b) Claesson, P. M.; Rutland, M. W. Measuring Interactions between Surfaces. In *Handbook of Applied Surface and Colloid Chemistry*; Holmberg, K., Ed.; Wiley: New York, 2001; pp 933−964.

(16) Raiteri, R.; Grattarola, M.; Butt, H. J. *J. Phys. Chem. B* **1996**, *100*, 16700−16705.

(17) (a) Crocker, J. C.; Grier, D. G. *MRS Bull.* **1998**, *23*, 24−31. (b) Resnick, A. *J. Colloid Interface Sci.* **2003**, *262*, 55−59.

(18) (a) Semmler, M.; Ricka, J.; Borkovec, M. *Colloids Surf. A* **2000**, *165*, 79−93. (b) Behrens, S. H.; Christl, D. I.; Emmerzael, R.; Schurtenberger, P.; Borkovec, M. *Langmuir* **2000**, *16*, 2566−2575. (c) Bouyer, F.; Robben, A.; Yu, W. L.; Borkovec, M. *Langmuir* **2001**, *17*, 5225−5231. (d) Behrens, S. H.; Borkovec, M.; Schurtenberger, P. *Langmuir* **1998**, *14*, 1951−1954.

(19) Wang, Z. L. Transmission Electron Microscopy and Spectroscopy of Nanoparticles. In *Characterization of Nanophase Materials*; Wang, Z. L., Ed.; Wiley−VCH: Weinheim, Germany, 2000; Vol. 1, pp 37−80.

(20) Liu, J. Scanning Transmission Electron Microscopy of Nanoparticles. In *Characterization of Nanophase Materials*, 1st ed.; Wang, Z. L., Ed.; Wiley−VCH: Weinheim, Germany, 2000; pp 81−132.

(21) Johnson, C. A.; Lenhoff, A. M. *J. Colloid Interface Sci.* **1996**, *179*, 587−599.

(22) Meurk, A.; Luckham, P. F.; Bergstrom, L. *Langmuir* **1997**, *13*, 3896−3899.

(23) Antelmi, D. A.; Spalla, O. *Langmuir* **1999**, *15*, 7478−7489.

(24) (a) Shin, E.-M.; Koenig, J. L. *Appl. Spectrosc.* **2002**, *56*, 1251−1258. (b) Cross, W. M.; Ma, S.; Winter, R. M.; Kellar, J. J. *Colloids Surfaces A* **1999**, *154*, 115−125.

(25) Jullien, R.; Meakin, P. *J. Phys. A: Math. Gen.* **1992**, *25*, L189−L194.

(26) Pagonabarraga, I.; Wojtaszczyk, P.; Rubi, J. M.; Senger, B.; Voegel, J.-C.; Schaaf, P. *J. Chem. Phys.* **1996**, *105*, 7815−7827.

(27) Adamczyk, Z.; Siwek, B.; Zembala, M.; Weronski, P. *Langmuir* **1992**, *8*, 2605−2610.

(28) Semmler, M.; Mann, E. K.; Ricka, J.; Borkovec, M. *Langmuir* **1998**, *14*, 5127−5132.

(29) Adamczyk, Z.; Warszynski, P. *Adv. Colloid Interface Sci.* **1996**, *63*, 41.

(30) Johnson, C. A.; Lenhoff, A. M. *J. Colloid Interface Sci.* **1996**, *179*, 587−599.

(31) Bohmer, M. R.; van der Zeeuw, E. A.; Koper, G. J. M. *J. Colloid Interface Sci.* **1998**, *197*, 242−250.